Earth, Planets and Space

FULL PAPER Open Access

Contribution to crustal strain accumulation of minor faults: a case study across the Niigata–Kobe Tectonic Zone, Japan

Tomonori Tamura[1*], Kiyokazu Oohashi[1], Makoto Otsubo[2], Ayumu Miyakawa[2] and Masakazu Niwa[3]

Abstract

Recent global navigation satellite system (GNSS) data for the Japanese Islands have revealed a high-strain-rate region suggesting the existence of a region of broad-scale crustal deformation. The Niigata–Kobe Tectonic Zone (NKTZ), which is the high-strain-rate zone in central Japan, shows a short-term dextral strain rate of ~12 mm/year. The total slip rate of the Quaternary fault zones in the NKTZ has been estimated as ~6.7 mm/year, accounting for just over half the short-term strain rate of the zone. However, this slip rate underestimates the total slip rate on faults within the NKTZ owing to possible distributed deformation on minor faults. This study quantifies the slip rate attributable to these other faults in the southeastern-central NKTZ and reveals the unique deformation structure across the high-strain-rate zone, which comprises a Quaternary fault core, a Quaternary fault damage zone, an incipient brittle shear zone (active background), and an inactive background. The spatial characteristics of the incipient brittle shear zone can be explained in terms of fault density, which increases toward the central NKTZ. Minor faults located > 500 m from major Quaternary faults but within the NKTZ have sense of shear consistent with that of the major faults. In contrast, minor faults outside of the NKTZ show sense of shear that differ from the dextral displacement of the high-strain-rate zone and do not contribute to the slip rate of the zone. The total slip rate of minor faults in the southeastern-central NKTZ is estimated to be 0.46–2.88 mm/year (roughly equal to a major Quaternary fault in the zone), which implies 4–24% of crustal strain is stored in the active background.

Keywords: Niigata–Kobe Tectonic Zone, Strain-rate paradox, Minor faults, Brittle shear zone, Slip rate

Introduction

The Niigata–Kobe Tectonic Zone (NKTZ; Sagiya et al. 2000) is one of the largest strain-concentration zones in Japan and extends from the northeastern (Niigata area) to southwestern (Kobe area) parts of Japan (Fig. 1a). Ohzono et al. (2011) demonstrated a dextral motion of ~12 mm/year across the NKTZ using dense GNSS observations. The NKTZ contains NE–SW-trending Quaternary fault zones (the Ushikubi, Atotsugawa, and Takayama–Oppara Fault Zones) whose orientation and sense of displacement are consistent with those of the NKTZ (Fig. 1b). Trench excavations and river terrace displacements indicate the long-term slip rates of these fault zones are 2–3, 1–2, and 1.7 mm/year, respectively (Headquarters for Earthquakes Research Promotion 2004). However, the total slip rate of these fault zones (~6.7 mm/year) is much lower than the slip rate obtained by GSNN observations (Ohzono et al. 2011). Assuming that the rate of crustal deformation is constant, a geodetic (short-term) slip rate of ~5.3 mm/year is unaccounted for. A discrepancy between geodesy and geology has also been reported in the eastern California shear zone (ECSZ), with the geodetic slip rate being 12 ± 2 mm/year and the geology-based long-term rate being 6.2 ± 1.9 mm/year (Dolan et al. 2007; Oskin et al. 2008; Chuang and Johnson 2011). This difference between

*Correspondence: i004wb@yamaguchi-u.ac.jp
[1] Graduate School of Sciences and Technology for Innovation, Yamaguchi University, 1677-1, Yoshida, Yamaguchi 753-8511, Japan
Full list of author information is available at the end of the article

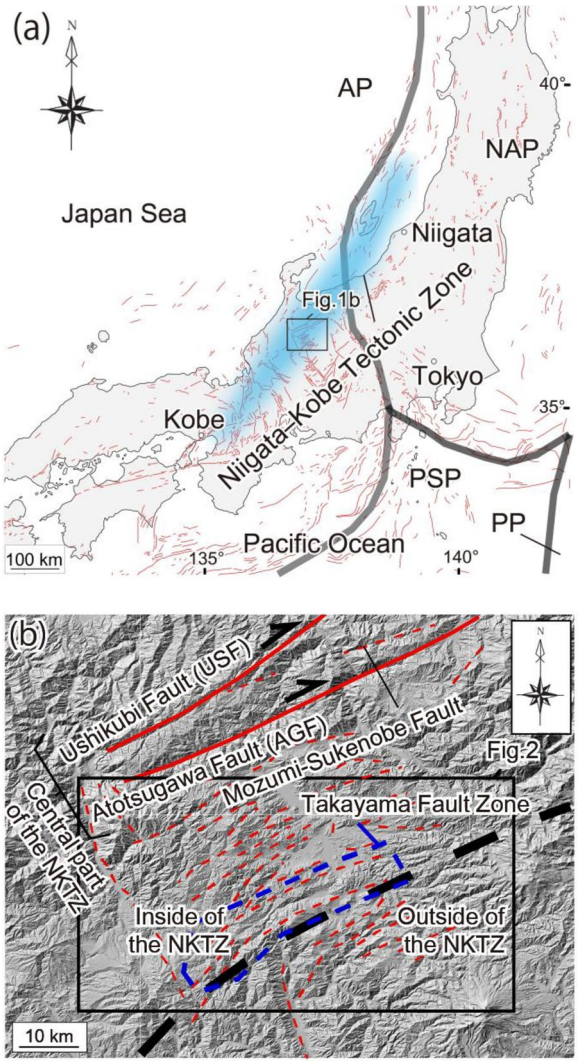

Fig. 1 The distribution of the Niigata–Kobe Tectonic Zone. **a** Major Quaternary faults and the NKTZ in Japan. The Japanese Islands are surrounded by the Japan Sea and the Pacific Ocean. The Japanese Islands lie on four plates: the Amurian plate (AP), the North American plate (NAP), the Philippine Sea plate (PSP), and the Pacific plate (PP) (e.g., Wakita 2013), with plate boundaries shown as thick black lines. Fine red lines indicate Quaternary faults as given by Research Group for Active Faults of Japan (1991). The blue region shows the distribution of the Niigata–Kobe Tectonic Zone (e.g., Sagiya et al. 2000). The small rectangle indicates the central NKTZ (**b**). **b** The Quaternary faults around the NKTZ. Solid red lines show the distribution of the major Quaternary faults (the Ushikubi Fault and the Atotsugawa Fault) in the central part of the NKTZ. Dashed red lines show the distribution of the Quaternary faults except the major Quaternary faults (the Ushikubi Fault and the Atotsugawa Fault) as given by Research Group for Active Faults of Japan (1991). Dashed blue box shows the distribution of the Takayama Fault Zone. Thick dashed black line shows the southern margin of the Takayama Fault Zone (we regarded it as the southern margin of the NKTZ). The black box is corresponding to the area of Fig. 2

the short-term and long-term slip rate (strain rate) is known as the "strain-rate paradox" (e.g., Sagiya and Meneses-Gutierrez 2016).

Strain-rate paradox has been debated for a long time. Wesnousky and Scholz (1982) showed a difference exceeding one order of magnitude in the moment-release rate between seismicity during the last 400 years and active faults in Japan. Consideration of elastic rebound theory (Reid 1910) with respect to the accumulation and release of stress and strain for crustal faults suggests that the short-term strain rate in an area surrounding faults should agree with the sum of the long-term slip rates of the faults. Crustal deformation triggered by infrequent, large-magnitude ($M \geq 9.0$) earthquakes is proposed as a possible explanation for the strain-rate paradox (Ikeda et al. 2012). For example, elastic strain in northeastern Japan crust was released during the 2011 Tohoku-Oki earthquake (Mw = 9) (Ikeda et al. 2012). This might result in the long-term strain rate (i.e., for periods greater than a few kyr, longer than the recurrence interval of great earthquakes) falling below the short-term strain rate (for periods of a few decades) (Ikeda et al. 2012). However, Angela-Menesses and Sagiya (2016) demonstrated continuity of E–W contraction in the NKTZ before and after the 2011 Tohoku-Oki earthquake by separating short- and long-wavelength components from GNSS data in the central Niigata region. Those authors inferred that this continuous strain state is related to aseismic slip of a deep crustal fault, which explained the existence of inelastic deformation in the NKTZ. Thus the strain-rate paradox in the NKTZ is still open question.

Ohzono et al. (2011) listed three possible reasons for the strain-rate paradox in the NKTZ: (1) inelastic deformation of the crust due to unaccounted-for minor faults and fractures; (2) the effects of volcanoes, and (3) viscous deformation of the lower crust. Because of the following reasons, we focus on the contribution of minor faults in the NKTZ which were not detected so far as the explanation of the crustal deformation. (I) In the NKTZ, paleomagnetic data suggest a broad deformation (dextral shear zone and/or block rotation) of Quaternary sediment adjacent to the Quaternary fault (Itoh et al. 2004; Kimura et al. 2004). (II) For the Ushikubi and the Atotsugawa Fault Zones in the NKTZ, Oohashi and Kobayashi (2008) and Niwa et al. (2011) found minor faults (ranging from a few millimeters to one centimeter in thickness) both within and outside of the fault damage zones. However, the structural characteristics and role of brittle deformation along the NKTZ remain unclear because the distribution, nature, displacement, and age of movement are unknown.

The purpose of this study is to quantify the contribution of strain accumulation of minor faults on the basis

of topographic and geological investigations. This study also establishes the characteristic features of deformation of the geodetically detected high-strain-rate zone of the NKTZ. In our study, we targeted the Inobuseyama and Kurumijima areas for field survey to find the minor faults (Fig. 2). The Inobuseyama area lies ~5 km southeast of the Atotsugawa Fault, which is situated in the central NKTZ. The Kurumijima area is ~40 km southeast of the Atotsugawa Fault and is located immediately to the southeast of the NKTZ. Here, we report (1) the Quaternary faults and lineaments across the NKTZ; (2) the density and nature of minor faults found in the central NKTZ (Inobuseyama area) and outside of the NKTZ (Kurumijima area) and (3) estimated slip rate of minor faults in the NKTZ.

Tectonic setting and geological background

The Japanese Islands are situated on or near the subduction margins of four plates: the Pacific, Amurian, North American, and Philippine Sea plates (Fig. 1). The Pacific plate is subducting beneath the North American and Philippine Sea plates, and the Philippine Sea plate is subducting beneath the Amurian Plate. The NE–SW-trending NKTZ of central Japan is 50–80 km wide and straddles the Amurian and North American Plates. Regions of high He^3/He^4 ratio aligned along the NKTZ suggest the ascent of fluids derived from dehydration of the subducting Philippine Sea plate, and the concentration of strain in the NKTZ may have arisen from the development of fluid-weakened lower crust (Iio et al. 2002). The existence of water in the upper and lower crusts of the NKTZ is also supported by seismic tomography (Nakajima and Hasegawa 2007).

The NKTZ comprises three NE–SW- to ENE–WSW-trending major fault zones, namely, the Atotsugawa, Ushikubi, and Takayama–Oppara Fault Zones. The Atotsugawa Fault Zone (AGF) has the highest level of seismic activity in the NKTZ and is the source fault of the 1858 Hietsu earthquake ($M=7.0$). Microseismicity has been detected along the Atotsugawa Fault Zone (e.g., Ito et al. 2007). Displacements measured from fault outcrops and trench excavations along river terraces have yielded

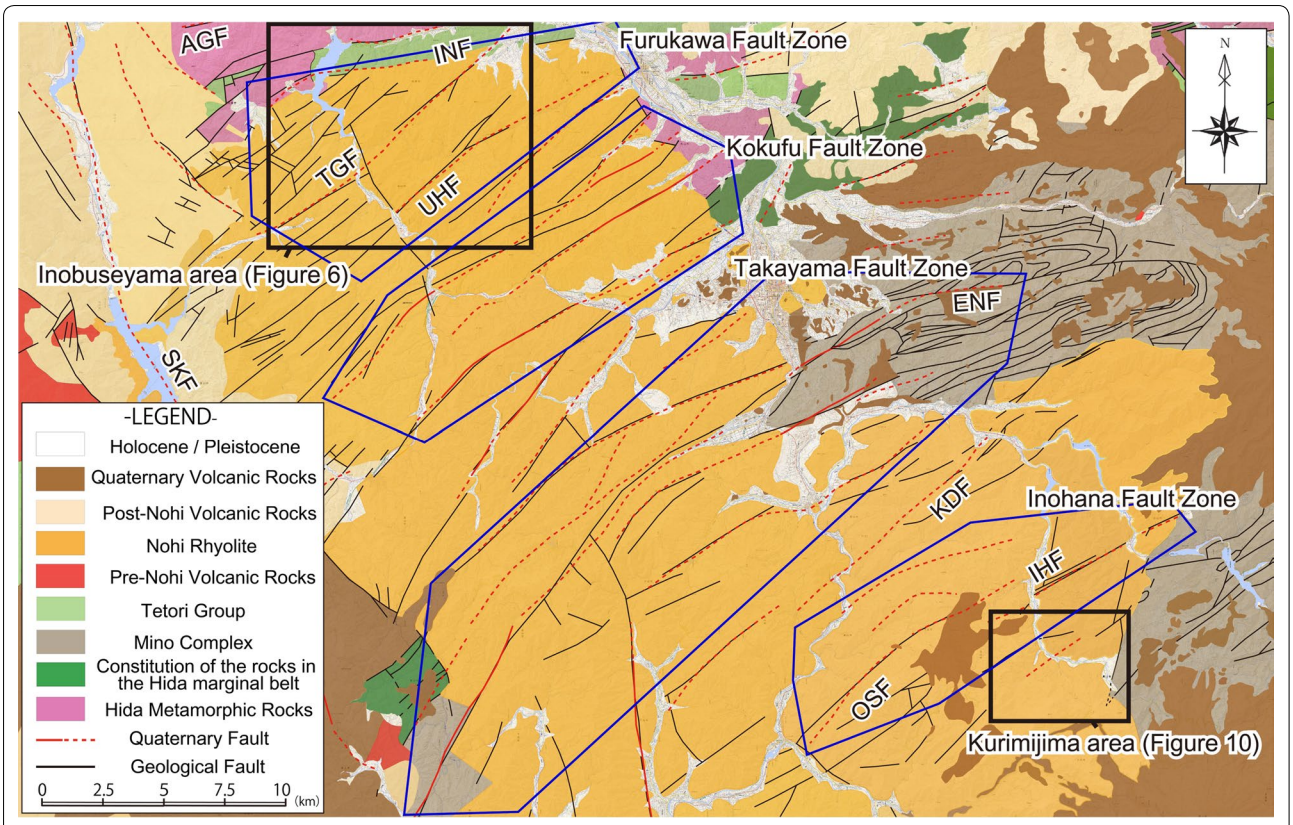

Fig. 2 Geological map of the southeastern-central part of the NKTZ and a region outside (to the southeast of) the zone, modified after Geoland Gifu (https://geo-gifu.org/geoland/gaikan/contents_top.html). Red lines are Quaternary fault traces or lineaments reported by Research Group for Active Faults of Japan (1991). The rectangles enclose the studied Inobuseyama and Kurumijima areas (see Figs. 6 and 10, respectively). Topographical map (1:25,000) is from the Geospatial Information Authority of Japan. *AGF* Atotusgawa Fault, *INF* Inagoe Fault, *TGF* Toichigawa Fault, *UHF* Unehata Fault, *SKF* Shirakawa Fault, *ENF* Enako Fault, *KDF* Kuchiudo Fault, *IHF* Inohana Fault, *OSF* Osaka Fault

a recurrence interval of 2500 years and an average dextral slip rate of 3.0–5.0 mm/year (Research Group for the Atotusgawa Fault 1989; Takeuchi et al. 2003). The Takayama–Oppara Fault Zones comprise the Furukawa, Kokufu, Takayama, and Inohana Fault Zones (Fig. 2; Headquarters for Earthquake Research Promotion 2004). The Furukawa Fault Zone contains the Inagoe, Toichigawa, and Unehata Faults, and the Inohana Fault Zone contains the Osaka and Inohana Faults. The Inagoe Fault shows clear evidence for faulting during the Quaternary, whereas the timing of the most recent activity on the other faults is unknown (Research Group for Active Faults of Gifu Prefecture 2008). An average dextral slip rate of 0.7 mm/year has been estimated for the Makigahora Fault in the Kokufu Fault Zone, on the basis of 2.5–3.0 m displacement of a 30-ka terrace (Gifu Prefecture 2001). The Takayama Fault Zone, which we regarded it as the southern margin of the NKTZ since the consistent horizontal velocity (less deformation) of the crust was observed around the Takayama Fault Zone according to Ohzono et al. (2011), has a slip rate of ~1.0 mm/year, as determined from 100 m displacement of a ~0.1 Ma river terrace along the Enako Fault (Gifu Prefecture 2001). In contrast, the Miboro Fault Zone, a NW–SE-trending major Quaternary fault zone in the NKTZ, has a sinistral sense of shear and does not contribute to the dextral motion of the NKTZ.

The broad-scale geology of the NKTZ is characterized by three major belts from north to south: the Hida belt (middle-to-late Paleozoic), the Hida marginal belt (Ordovician to Cretaceous), and the Mino belt (Late Triassic to Early Cretaceous) (e.g., Isozaki et al. 2010; Wakita 2013). The Hida belt comprises metamorphic rocks (gneiss), marble and granites; the Hida marginal belt is composed of metamorphic rocks, granites, and sedimentary rocks; and the Mino belt consists mainly of sedimentary rocks. The Nohi rhyolite (late Cretaceous rhyolite, tuff breccia, and tuff) is widespread in the NKTZ (Fig. 2). The Nohi rhyolite, the Hida metamorphic rocks, and the Tetori Group (late Jurassic to early cretaceous mudstone, sandstone, and conglomerate) occur in the Inobuseyama area (Nozawa et al. 1975). The Kurumijima area contains the Nohi rhyolite and the Suzuran–Kognen basalts (early Pleistocene), and granites are intruded into the Nohi rhyolite (Yamada et al. 1985).

Methods

To understand the distribution and density of the Quaternary faults and lineaments both inside and outside the NKTZ, we conducted topographic analysis using aerial photography. We mapped the Quaternary faults and lineaments using 1:10,000–1:20,000-scale aerial photographs taken by the Geospatial Information Authority of Japan (GSI), for which the resolution is higher than those used in previous studies (1:20,000–1:50,000-scale aerial photographs; Research Group for Active Faults of Japan 1991; Suzuki and Sugito 2010). In cases where landforms were unclear because of anthropogenic modification, older and lower-resolution aerial photographs (1:40,000) were used. The aerial photograph analysis was conducted for an area extending from the central part of the zone to its southeastern margin, between Inobuseyama and Kurumijima area (Fig. 3). Detected traces were subdivided into three groups according to the certainty of detection (Quaternary faults, presumed Quaternary faults, and lineaments), which is following the guidelines of Nakata and Imaizumi (2002) and Takada et al. (2003). While Nakata and Imaizumi (2002) defined Quaternary faults (site indistinct) as one of the groups, we did not use this category since the study area is hardly affected by anthropogenic modifications. Although lineaments are subdivided into two groups according to their clarity based on Takada et al. (2003), we regarded them as "lineaments" of a group in this paper. Quaternary faults are assigned to a fault when it is certain that the fault was active during the Quaternary and thought that it is activated repeatedly in the past (clear evidence exists for the amount and sense of displacement). Presumed Quaternary faults are assigned when we locate the trace of the tectonic landforms (the sense of displacement can be also inferred), but we could not clearly recognize their activation during the Quaternary. Lineaments are assigned when we could find linear topographies with unclear displacement markers (or without any displacement markers), which is also suspected of being active during the Quaternary. To determine and understand the variation in areal density of the Quaternary faults and lineaments in and around the NKTZ, the total length of the Quaternary faults and lineaments per unit area was calculated for 2-dimensional subareas (cells) over the studied area (Fig. 3b). Because the density of faults might be affected by host rock rheology (i.e., rock strength), we compared densities of the Quaternary faults and lineaments in subareas of the same lithology, namely, the Nohi rhyolite (cells enclosed by the red polygon in Fig. 3b).

We also investigated the Inobuseyama and Kurumijima areas in the field, identifying minor faults (millimeter- to meter-width scale) and mapping their distribution, and describing other features of the associated fault core (e.g., strike, dip, striations, width and type of fault rock, and deformation structures). Fault displacements were obtained by measuring faults widths and converting them to displacements according to an empirical relationship (see "Discussion" for details). Moreover, we applied

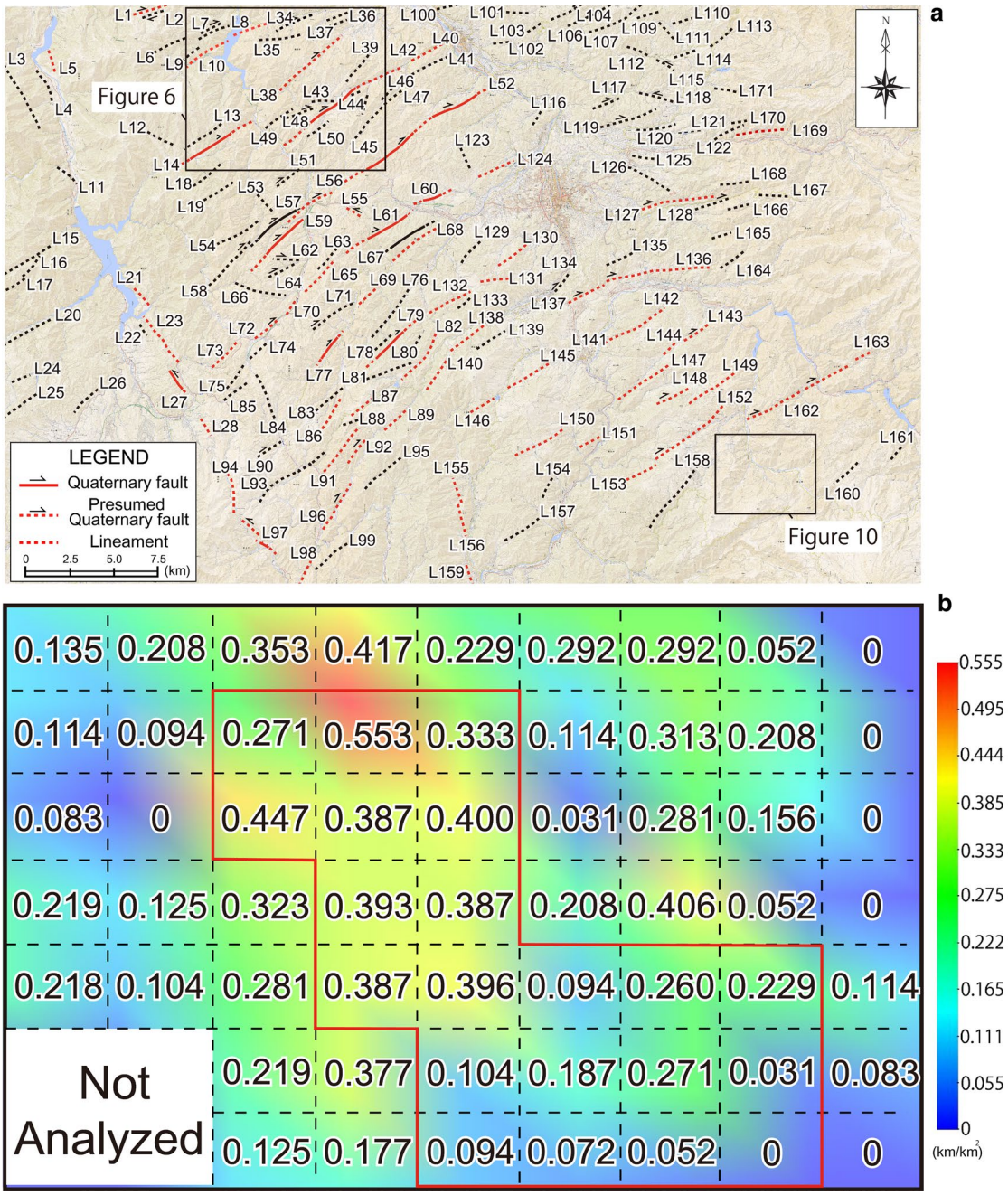

Fig. 3 Fault traces and lineaments in the southeastern-central NKTZ and to the southeast of the zone. **a** Distribution of fault traces and lineaments in the study area. Red lines and black lines show fault traces and lineaments detected in this study that are consistent and inconsistent with the distribution of Quaternary fault traces reported by Research Group for Active Faults (1991), respectively. The rectangles indicate the studied Inobuseyama and Kurumijima areas (see Figs. 6 and 10, respectively). **b** Fault traces and lineament densities in kilometers per unit area (1 km^2). The polygon enclosed by the red lines indicates the area covered mainly by the Nohi rhyolite. The 1:25,000-scale topographic map is from the Geospatial Information Authority of Japan

the multiple inverse method (Yamaji 2000; Yamaji et al. 2011) and the *k*-means clustering method (Otsubo et al. 2006) to slip data obtained in the Inobuseyama area to determine the orientations of paleostress fields.

Results

Distribution of Quaternary faults, presumed Quaternary faults and lineaments

From our detailed aerial photograph analysis and

interpretation, we recognized 171 Quaternary faults (hereafter, we refer "Quaternary faults and presumed Quaternary faults" as "fault traces") and lineaments in the study area (Fig. 3a). The number of Quaternary faults, presumed Quaternary faults, and lineaments was 11, 31, and 129, respectively. The number of Quaternary faults was slightly lower than that of a previous inventory, which identified 13 faults (Certainty I; Research Group for Active Faults of Japan 1991). The majority of the detected Quaternary faults correspond to Certainty I identified by previous studies (Research Group for Active Faults of Japan 1991; Suzuki and Sugito 2010). Our study showed presumed Quaternary fault traces of L92 and L96 with right-lateral offsets of ridges and streams. On the other hand, the Research Group for Active Faults of Japan (1991) showed the Certainty I (the Quaternary fault, not the presumed Quaternary fault) along the fault traces of L92 and L96 since they referred the fault outcrops previously recognized (Tsuneishi 1976) as an evidence of the activity. However, Tsuneishi (1976) did not recognize the evidence of the activity during the Quaternary in its fault descriptions. Therefore, the discrepancy of the number between this study (Quaternary faults) and previous inventory (Certainty I) may reflect a slight overestimation of Research Group for Active Faults of Japan (1991).

The number of presumed Quaternary fault increased from the previous inventory of 19 (Corresponding to Certainty II; Research Group for Active Faults of Japan 1991) to 31 (Fig. 3a). Some of these traces are located along Quaternary fault traces detected by previous studies (Research Group for Active Faults of Japan 1991; Suzuki and Sugito 2010), whereas others are newly recognized. Lineaments increased drastically from the previous inventory of 39 (Certainty III which is suspected Quaternary faults or lineaments; Research Group for Active Faults of Japan 1991) to 129 (Fig. 3a). The fault traces were identified mostly in the area near the Atotsugawa Fault (0–20 km), whereas lineaments were recognized mostly at distance from the Atotsugawa Fault (20–40 km; Fig. 3a). The fault traces and lineaments were not detected in the eastern/southeastern part of the study area (Fig. 3). Such traces may not have been detected because of the Norikura volcanics, which form the Quaternary geology of the eastern part of the study area. These young rocks might have obscured the tectonic expression of minor faults unless there was considerable repeated fault activation after the volcanism. The resultant relationship shows that density of fault traces and lineaments decreases with increasing distance from the Atotsugawa Fault and from the central part of the NKTZ (Fig. 1b and L1 in Fig. 3a).

The fault traces and lineaments are oriented NE–SW and NW–SE (Fig. 4). The NE–SW-trending fault traces and lineaments are distributed in the central part of the study area, whereas the NW–SE-trending fault traces and lineaments tend to appear locally around the western part. Displaced rivers and river terraces indicate dextral movement on the NE–SW-trending fault traces and lineaments, and sinistral movement on the NW–SE-trending fault traces and lineaments. This implies that the maximum principal stress, σ_1, is oriented E–W and the minimum principal stress, σ_3, is oriented N–S, which is consistent with the present stress field in central Japan (Katsumata et al. 2010; Imanishi et al. 2011; Tsutsumi et al. 2012). The locations or strikes of Quaternary faults in the Inobuseyama area (e.g., the Inagoe, Toichigawa, and Unehata Faults) are consistent with those of

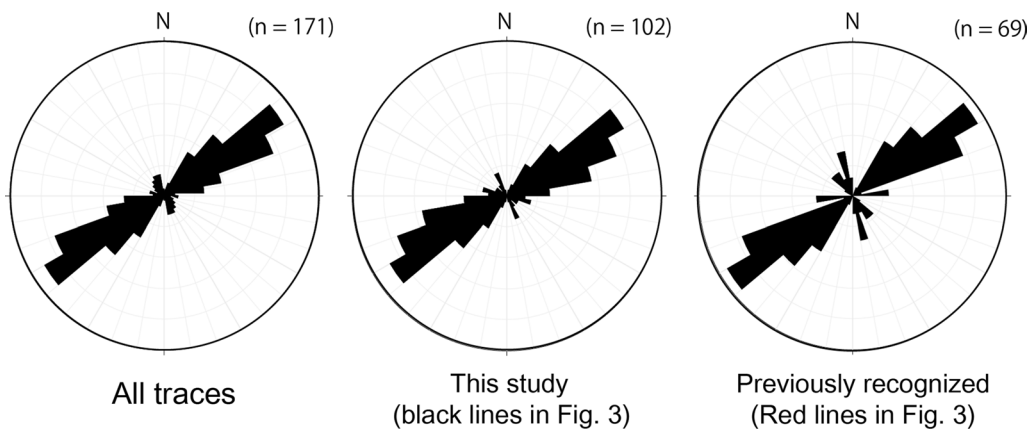

Fig. 4 Rose diagrams showing the orientations of the identified fault traces and lineaments. Left: all traces; center: fault traces and lineaments newly detected in the present study; right: fault traces and lineaments detected in previous studies (including Research Group for Active Faults 1991; Suzuki and Sugito 2010)

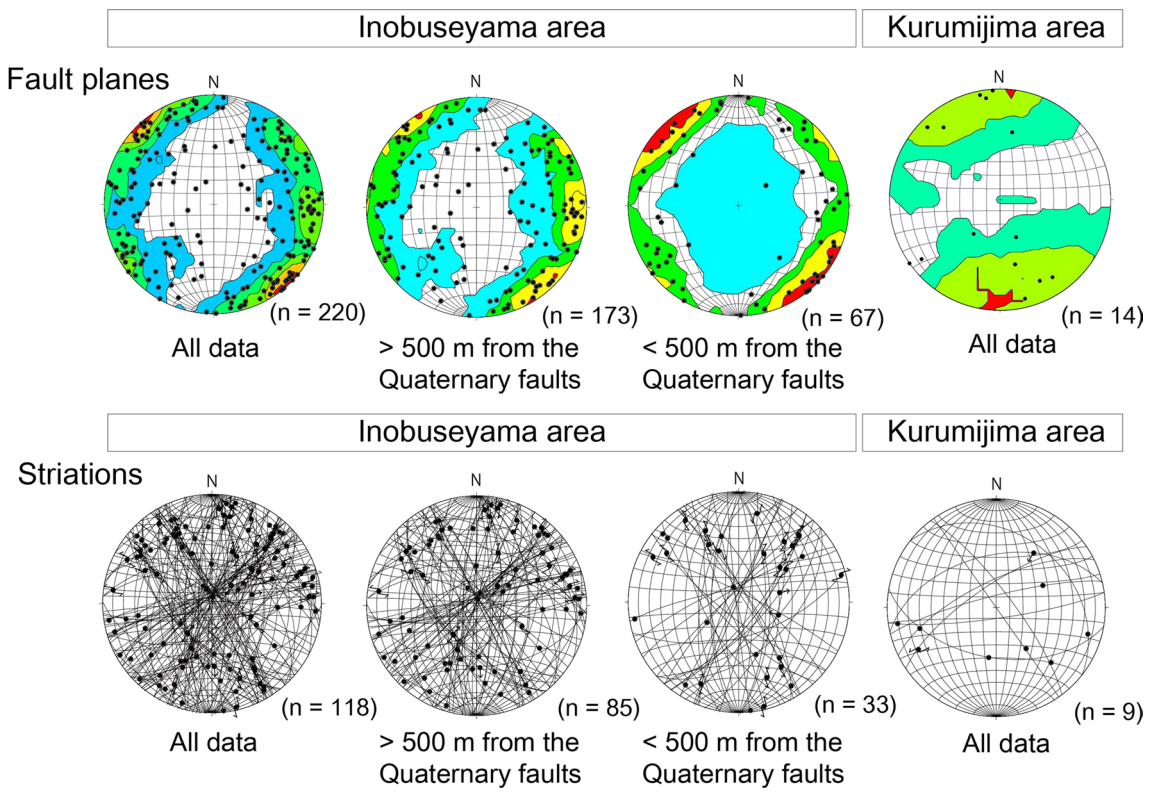

Fig. 5 Lower-hemisphere, equal-area stereographic projections showing poles to fault planes and the orientations of fault planes and the plunges of striations on fault planes in the Inobuseyama and Kurumijima areas

geological faults or minor faults (Figs. 4, 5 and 6). However, the N–S- and E–W-trending geological faults do not show any clear evidence of activity as inferred from topographic analysis. These results suggest that the NE–SW-trending Quaternary faults are geological faults that have been reactivated in response to the E–W compressional stress field.

Fault occurrence

Inobuseyama area

A total of 220 faults trending mostly NE–SW, NW–SE, and N–S were recognized during the field survey in the Inobuseyama area (Figs. 5 and 6). Faults in this area commonly contain a fault gouge and/or fault breccia. Six fault gouges with a thickness of > 10 cm were found on fault traces and lineaments identified from aerial photographs and geological faults, except for one fault outcrop whose fault gouge and breccia zone was 10–20 cm in width located to the south of Miborotani (Figs. 6 and 7). In contrast, small-scale faults measuring millimeters to a few centimeters in width, which were not sometimes detected in the aerial photo interpretations ("minor faults" hereafter), are also found in areas at distance (> 500 m) from the fault traces, lineaments and from geological faults. Most of the striations on these minor faults plunge at low to moderate angles on steeply dipping fault planes (Fig. 5).

At an outcrop that shows the core of the Unehata Fault, which has the largest fault width in the study area, the fault strikes N60°–65°E, shows a dextral sense of shear, and is marked by a gouge zone that is 30 cm thick (Figs. 7 and 8a, b). The region of the < 500 m away from Unehata Fault contains relatively thick (4.0–20.0 cm; Fig. 8c) NE–SW-trending fault gouges, although most of the faults in this damage zone are 0.1–1.0 cm thick (Fig. 7). The composite planar fabrics show a dextral sense of shear, consistent with the fault core (Fig. 8c). In contrast, only faults measuring 0.1–1.0 cm in width are found outside the damage zone (Fig. 8d). In addition, the orientations of the minor faults are similar to those of the Quaternary faults, trending mostly NE–SW to E–W (Fig. 5). Slickensteps and grooves on the slip surfaces, as well as the composite planar fabric in the fault rocks, indicate dextral displacement for the NE–SW- to ENE–WSW-striking faults and sinistral displacement for the NW–SE-striking faults (Fig. 8d). These senses of shear of minor faults (millimeter- to meter-in width) are consistent with those of the fault traces and lineaments, implying recent slip on these faults, as described below.

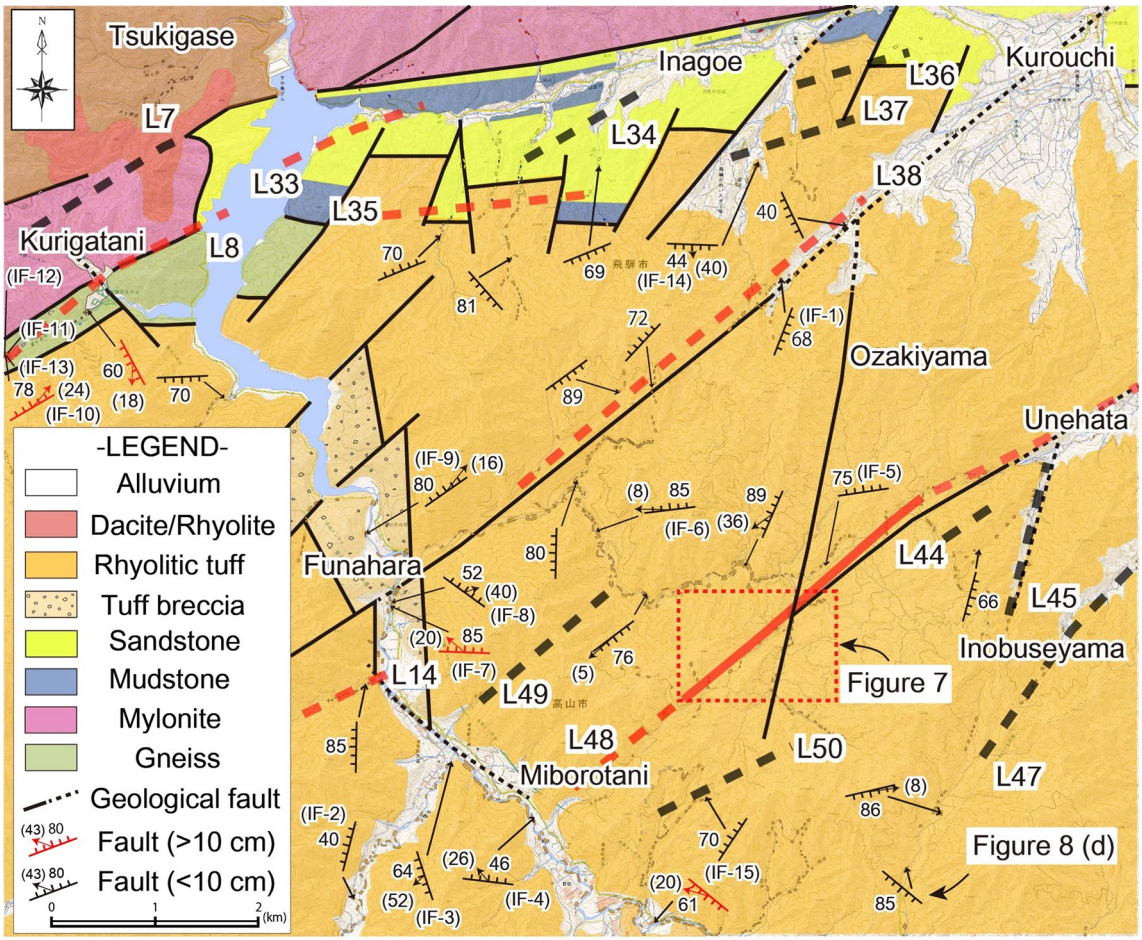

Fig. 6 Geological map (after Nozawa et al. 1975) and locations of the fault outcrops of the Inobuseyama area. Pale-red and black lines are fault traces and lineaments detected by aerial photograph analysis (shown in Fig. 3). The dashed red rectangle indicates the investigated area around the Unehata Fault (see Fig. 7). The 1:25,000-scale topographic map is from the Geospatial Information Authority of Japan

To clarify the timing of slip on all faults in the Inobuseyama area, we calculated the paleostress field from fault plane data. The entire slip data ($n=46$) show σ_1 directed E–W to ESE–WNW and σ_3 directed N–S to NNE–SSW (Fig. 9), which is consistent with the present stress field (Katsumata et al. 2010; Imanishi et al. 2011; Tsutsumi et al. 2012). This paleostress field from the entire slip data is expected to show the present stress field, as these data include the Quaternary faults that were detected from aerial photographs. We then applied the data outside the damage zones ($n=25$) to exclude the effect of these faults. Slip data for faults located outside the damage zones of the Quaternary faults (i.e., >500 m from the faults) show σ_1 directed E–W to ESE–WNW and σ_3 directed N–S to NNE–SSW (Fig. 9). This paleostress field is consistent with that for the pooled data. Therefore, minor faults in the Inobuseyama area have moved under the present stress field regardless of their distance from the Quaternary faults.

Kurumijima area

A total of 14 faults containing fault gouge and/or fault breccia were recognized during the field survey in the Kurumijima area (Fig. 10). These faults strike NE–SW to ENE–WSW, which is consistent with the strike of the NKTZ (Fig. 5). In contrast to Inobuseyama, faults striking N–S were not detected. Striations on the fault planes of minor faults show shallow to moderate plunges on steeply dipping fault planes (Fig. 5). Except for three minor faults located in the central Kurumijima area (Sokubotani; KF-5, KF-6, and KF-7), all of minor faults are found within ~500 m of geological faults. Their widths range from a few millimeters to a few centimeters with the exception of fault KF-1 in the northwestern part of the Kurumijima area. KF-1 is interpreted as the fault core of a NE–SW-trending geological fault and shows the thickest fault gouge zone (10 cm in width) in the area (Fig. 11a). The orientation of the gouge zone is N56°E/73°N and striations plunge 20° to the west.

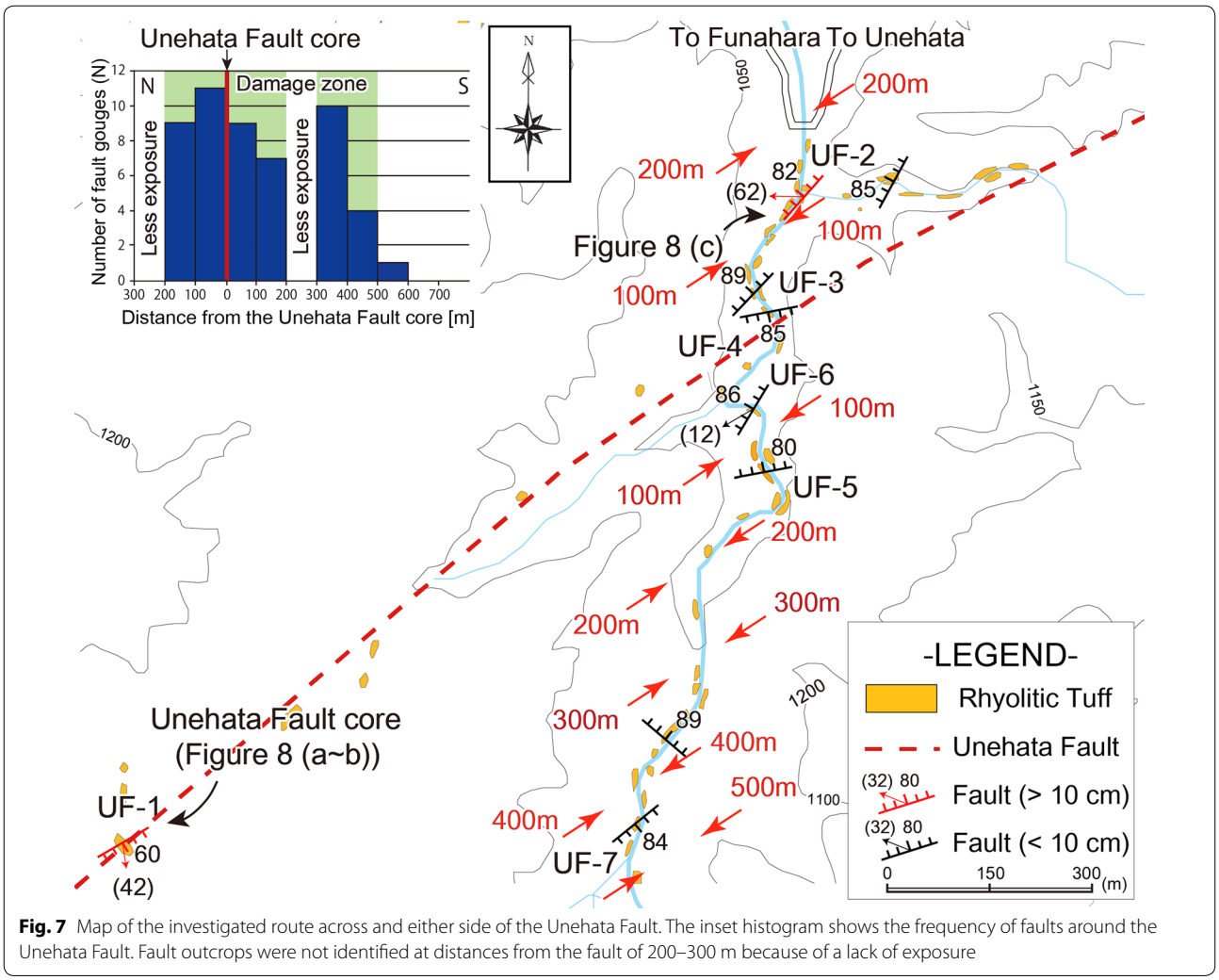

Fig. 7 Map of the investigated route across and either side of the Unehata Fault. The inset histogram shows the frequency of faults around the Unehata Fault. Fault outcrops were not identified at distances from the fault of 200–300 m because of a lack of exposure

Slip-surface features (comet marks) indicate sinistral–normal oblique slip. At an outcrop located 250 m from the nearest geological fault, a minor fault (KF-2) is oriented N77°E/50°N, contains a gouge zone that is ~1 cm wide (Fig. 11b, c), and the fault plane contains striations plunging 39° to the north. The composite planar fabrics of the fault gouge indicate sinistral–reverse oblique slip (Fig. 11d).

Two minor faults (KF-3 and KF-4) located ~500 m from geological faults in the northwestern part of the area trend NE–SW and are marked by gouge zones varying in width from a few millimeters to about one centimeter. Although the shear sense of these faults could not be identified, the striations on the fault planes plunge at moderate angles, indicating that these are oblique-slip faults. Minor faults in the central part of the area (KF-5, KF-6, and KF-7) strike ENE–WSW or NW–SE and are marked by zones of fault gouge that are a few millimeters wide. The striations on the fault plane of KF-7 plunge at moderate angles, whereas those on the fault planes of KF-5 and KF-6 could not be observed.

In contrast to the Inobuseyama area, we do not find any faults in the Kurumijima area that are consistent with the present stress field (i.e., we found no NE–SW-trending faults with a dextral sense of shear or NW–SE-trending faults with a sinistral sense of shear). This implies that the faults in the Kurumijima area were activated under a different stress field from that of the present day, possibly before the Quaternary.

Discussion

Slip rate in the NKTZ

To determine an overall slip rate (shear strain rate) for a specific area, information on the displacement and timing of slip is required for all faults in the area. However, obtaining this information directly, especially for minor faults, is essentially impossible in the present study area because of the lack of displacement markers and datable

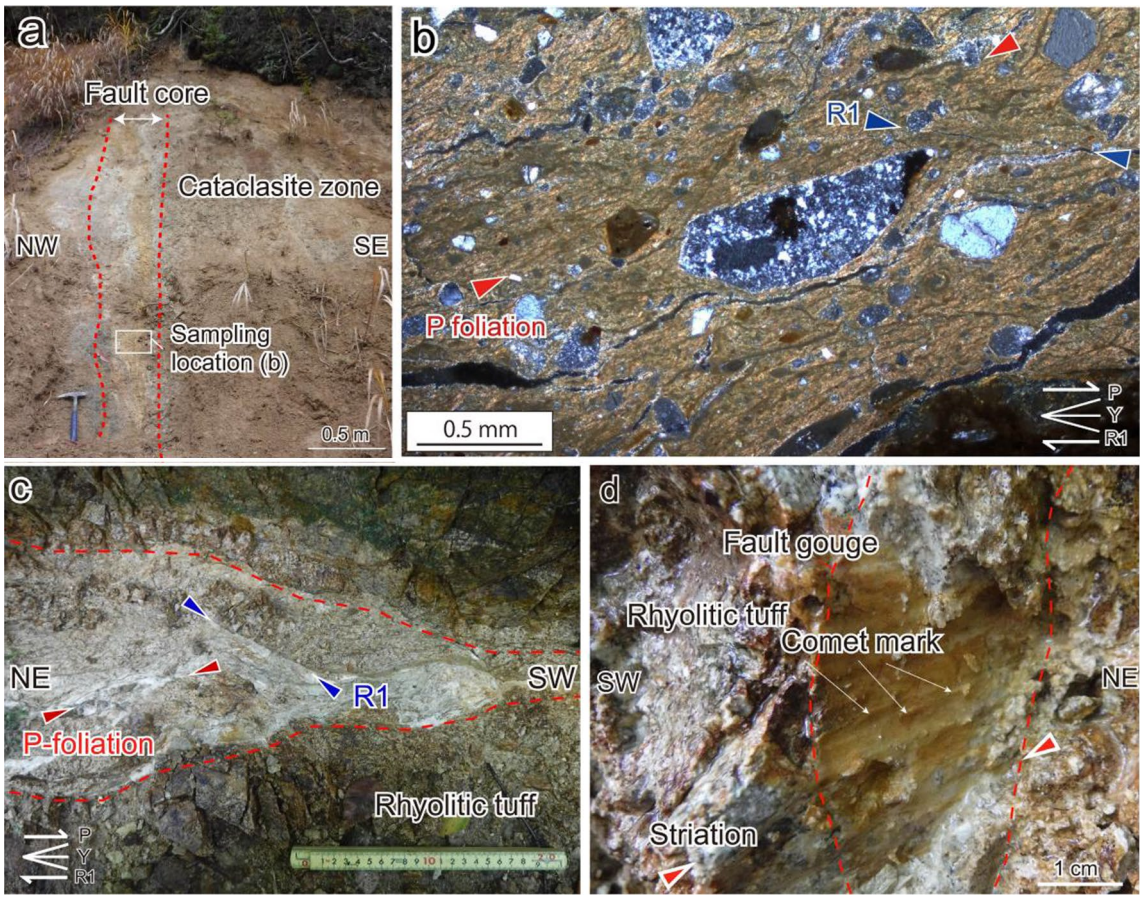

Fig. 8 Fault outcrops and fault materials in the Inobuseyama area. **a** Outcrop photograph of the core of the Unehata Fault. **b** Photomicrograph of fault gouge of the Unehata Fault. **c** Outcrop photograph of the zone of fault gouge and breccia of the Unehata Fault. **d** Outcrop photograph of a minor fault outside of the damage zone. R1 = Riedel shear; Y = Y plane; P = P-foliation of composite planar fabric

overlying sediments although the direct measuring of the displacement is common for quantifying the slip rate. We therefore quantified fault displacements in the Inobuseyama area (subarea A_1 in Fig. 12) by using an empirical relationship between the width and displacement of faults (e.g., Shipton et al. 2006; Childs et al. 2009; Fossen 2010). We then used this relationship to estimate the displacement in other subareas (subareas A_2, A_3, and A_4 in Fig. 12) by extrapolating the relationship between the total width of minor faults detected in the field and the density of topographically detected fault traces and lineaments in the Inobuseyama area. Finally, we obtained the slip rate of the NKTZ by dividing the total displacement of faults in the central to southeastern part of the NKTZ (the Atotsugawa Fault to southeastern margin of the NKTZ; A_1 A_2 A_3 and A_4 in Fig. 12) by the duration of Quaternary fault activity established in an adjacent area.

The total displacement on faults in the Inobuseyama area can be estimated by summing the widths of faults in the area (route map in Fig. 12). To sum up the widths (i.e., displacement) of faults contribute to the dextral motion of the NKTZ, we have to measure them along the line in the transverse direction (baseline) in the same manner with GNSS observation. Since the entire region of the Inobuseyama area has not been surveyed in this study, we extrapolate the obtained fault data along the investigated route to the unsurveyed area, based on the ratio of the total surveyed routes to a baseline. Here, we set a baseline (L_a, 9.75 km long; Fig. 12) oriented N30°W, perpendicular to the NKTZ, onto which points along the investigated routes were projected. The projected total length of these routes (red sections of the baseline in Fig. 12; L_1–L_5) is 7.95 km, whereas that of the unsurveyed area is 1.8 km. We then projected the fault population along the surveyed route onto the baseline (L_1, L_2, L_3, L_4 and L_5). Finally, we obtained the total fault width in the Inobuseyama area (W_{Iby}) by assuming that the ratio of the total surveyed routes (L_1, L_2, L_3, L_4 and L_5) to the baseline (L_a) is consistent with the ratio of the total

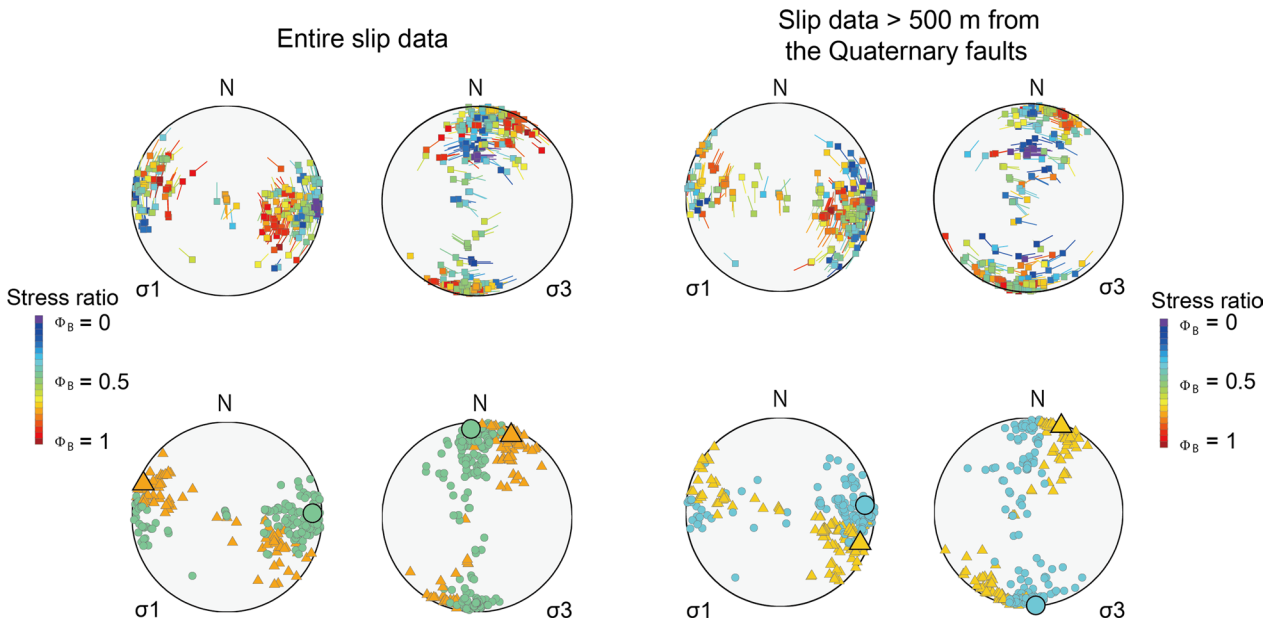

Fig. 9 Paired stereonets of slip data in the Inobuseyama area showing results of the multiple inverse method and *k*-means clustering. Upper plots show results obtained using the multiple inverse method (Yamaji 2000), and lower plots show results obtained using the *k*-means clustering (Otsubo et al. 2006). The circles and triangles in the stereo of lower side are cluster centers

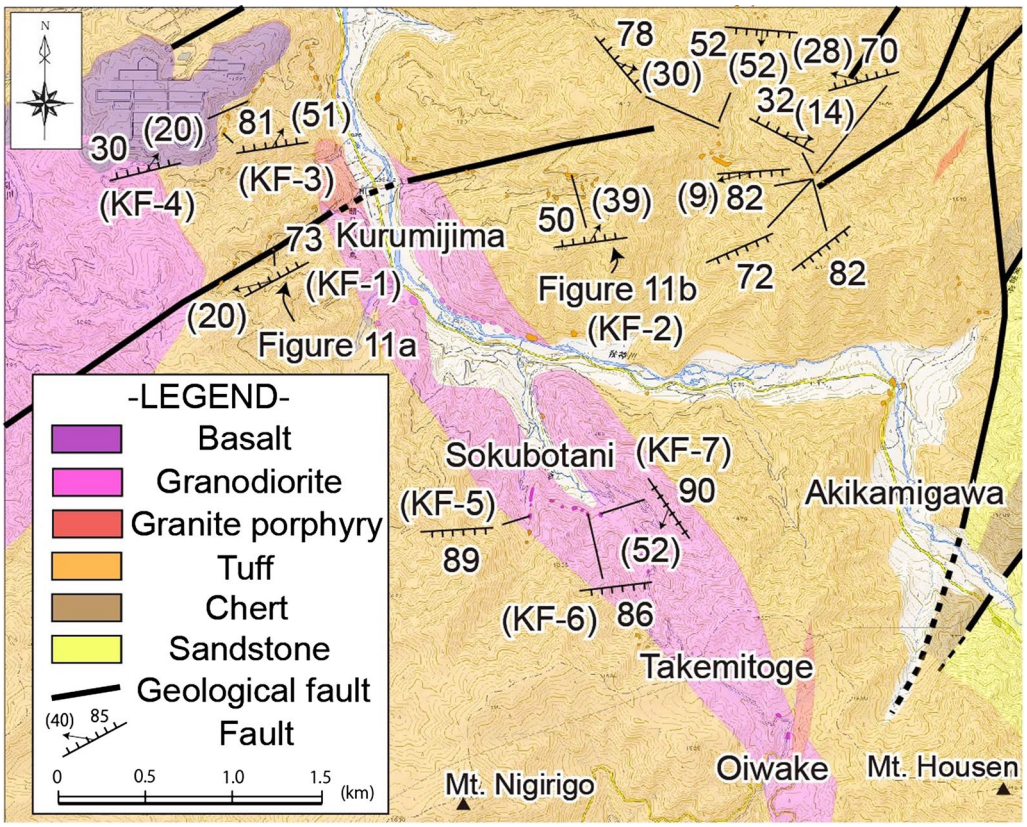

Fig. 10 Geological map of the Kurumijima area, modified after Yamada et al. (1985), showing the locations of fault gouge. The 1:25,000-scale topographic map is from the Geospatial Information Authority of Japan

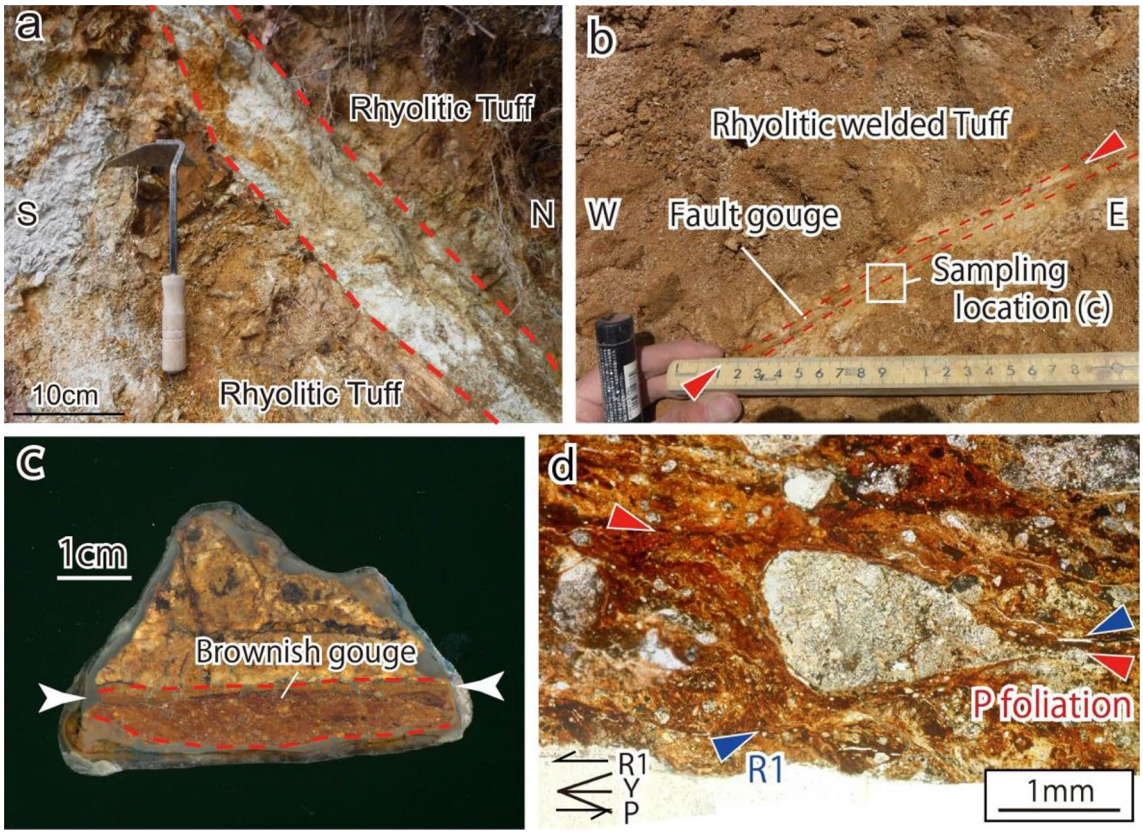

Fig. 11 Fault outcrops and fault materials in the Kurumijima area. **a** Photograph of the core of the geological fault. **b** Outcrop photograph of a minor fault (KF-2; N77°E/50°N) in the Kurumijima area. **c** Hand-specimen photograph of a sample from the outcrop shown in **b**. **d** Photomicrograph (light-polarized light image) of the fault gouge sample shown in **c**. R1 = Riedel shear; *Y* = *Y* plane; P = P-foliation of composite planar fabric

measured width of faults (W) to total fault width in the Inobuseyama area (W_{Iby}).

Before we extrapolate the obtained fault data to the unsurveyed area, we have to confirm the constant scaling properties (fractal geometry) of faults are satisfied in the study area. Cello et al. (2000) and Otsuki et al. (2005) confirmed that the linear relationships between cumulative number and fault width in a range of 2–3 orders of magnitude on log–log diagrams, which indicating self-similar (scale independent) properties of the faults. The faults in the Inobuseyama area also show a linear relationship between cumulative fault number and fault width (Fig. 13) over three orders of magnitude, suggesting that the faults in the NKTZ are considered to be self-similar in a range of outcrop to map scale. Thus, we consider the constant scaling properties of the fault in the NKTZ, which allowed us to assume that faults with same spatial properties are also distributed not only in the investigated area, but also in the uninvestigated area.

Although the faults that can explain the dextral motion of the NKTZ should trend ~N60°E, faults corresponding to the R1- and P-shears in composite planar fabrics (e.g., Chester and Logan 1987) should also contribute to the dextral motion. Therefore, N30°E- to N90°E-trending faults were also included in the analysis. The summed fault width along the investigated routes (W) is 3.73 m and the total fault width of the faults in the Inobuseyama area (W_{Iby}) is 4.57 m, calculated as follows:

$$W_{\mathrm{Iby}} = \frac{L_{\mathrm{a}} W}{L_1 + L_2 + L_3 + L_4 + L_5}, \tag{1}$$

where L_{a} and $L_1+L_2+L_3+L_4+L_5$ are the length of the baseline ($L_{\mathrm{a}}=9.75$ km) and total investigated route in the Inobuseyama area (red lines in Fig. 12; $L_1+L_2+L_3+L_4+L_5=7.95$ km), respectively. As the faults in the Inobuseyama area correspond closely to the detected fault traces and lineaments, we assumed that the density of fault decreases with increasing distance from the center of the NKTZ in the same manner as the topographically detected features. By assuming that the ratio of the density of the fault traces and lineaments in the Inobuseyama area (D_1) to that of the respective areas (D_2, D_3 and D_4) is consistent with the ratio of the total fault width in the

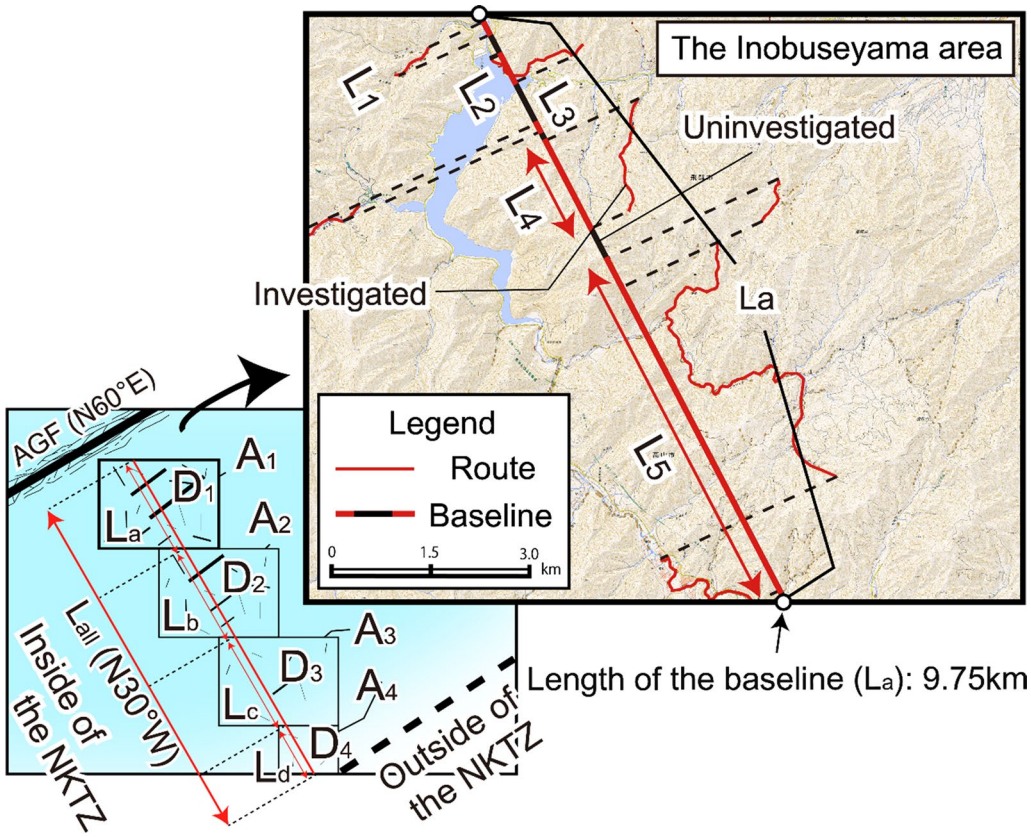

Fig. 12 Calculation of slip rate by using the analyzed transect and investigated route. The baseline (thick red/black line) in the route map is the line onto which the results of the geologically investigated route (thick red line) are projected. The blue zone in the measurement schematic diagram depicts the area inside the NKTZ, and the white zone represents the area outside the NKTZ. The thick black line represents the Atotsugawa Fault (AGF) located in the central NKTZ. The northwestern area (A_1) in the measurement schematic diagram corresponds to the Inobuseyama area

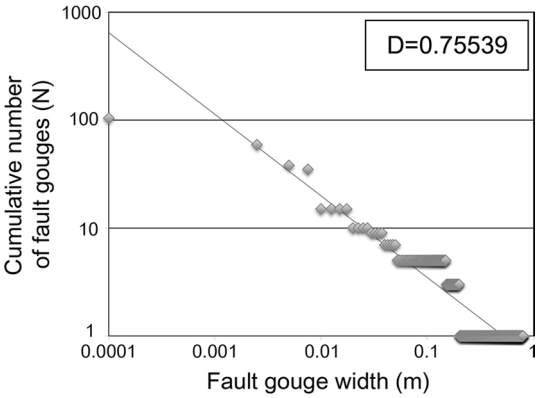

Fig. 13 Log–log plot of the cumulative number of fault gouges versus fault gouge width. The orientations of fault gouge planes and fault surface striations in the Inobuseyama and Kurumijima areas are shown in stereoplots

Inobuseyama area (W_{Iby}) to that of the study area (W_{total}), the total fault width of the respective areas was calculated as follows:

$$W_{\mathrm{total}} = \frac{D_2}{D_1} W_{\mathrm{Iby}} + \frac{D_3}{D_1} W_{\mathrm{Iby}} + \frac{D_4}{D_1} W_{\mathrm{Iby}} + W_{\mathrm{Iby}}, \quad (2)$$

where D_1–D_4 ($D_1 = 1.59$, $D_2 = 1.57$, $D_3 = 0.78$ and $D_4 = 0.072$) are the densities of fault traces and lineaments in corresponding subareas A_1–A_4. We obtained a value of $W_{\mathrm{total}} = 11.51$ m.

Previous studies of the relationship between fault displacement and width have shown that displacements are statistically 100 times greater than widths while the empirical equation contains one order of the displacement variation (e.g., Fossen 2010). Assuming that this relationship applies to faults in the southeastern-central NKTZ, the total displacement of all faults across the entire study area is estimated to be 1151 m.

The duration of slip upon minor faults in the NKTZ also needs to be clarified. The multiple inverse method

yielded a paleostress field with σ_1 oriented E–W to ESE–WNW and σ_3 oriented N–S to NNE–SSW (Fig. 9), suggesting that faults in the Inobuseyama area have moved in accordance with the present stress field (e.g., Katsumata et al. 2010; Imanishi et al. 2011; Tsutsumi et al. 2012). This implies that these faults have been active during the Quaternary (since ~ 2.5 Ma), as the present stress field in SW Japan is considered to have been established during the early Quaternary (e.g., Taira 2001). Matsuda et al. (2004) suggested that dextral movement on the Atotsugawa Fault was initiated more recently, between 1.5 and 0.4 Ma, on the basis of topographic offsets and average slip rate calculations. Therefore, the slip rate of the southeastern-central NKTZ is estimated to be 0.46–2.88 mm/year based on a total displacement of 1151 m and a slip duration of 0.4–2.5 Myr.

The total slip rate of the major Quaternary faults (the Atotsugawa, Ushikubi, and Takayama–Oppara Fault Zones) is 6.7 mm/year, and that of minor faults in the study area is 0.46–2.88 mm/year, which is nearly equal to the slip rate of the Atotusgawa or Uahikubi Fault Zones. This value gives a total rate for the NKTZ of 7.2–9.6 mm/year, accounting for 60–80% of the total strain rate observed in the NKTZ (12 mm/year). Thus, although accounting for minor faults in the NKTZ helps to close the deformation budget, around one-third of the deformation in the NKTZ remains unaccounted for. Slip rates of faults in the northern NKTZ still need to be determined, and minor faults have been recognized in field investigations in this part of the NKTZ (e.g., Oohashi et al. 2016). Further investigation in the northern NKTZ will allow an evaluation of the slip rates of faults in the region, and thereby we can evaluate how much the total slip rate of all faults in the NKTZ can account for the strain rate of the zone. In addition, the effects of volcanoes and viscous deformation of the lower crust as further explanations of the unaccounted-for strain are also listed (e.g., Ohzono et al. 2011). Therefore, it is important to consider those effects for evaluating the exact amount as the deformation in the NKTZ.

Relationships between fault traces, minor faults, and deformation in the NKTZ

In the Inobuseyama area, minor faults occur far from large-scale faults such as Quaternary faults or geological faults, and cannot be explained with the conventional fault zone models (fault core, damage zones and country rocks; e.g., Chester and Logan 1987; Mitchell and Faulkner 2009). In general, the internal structure of a fault comprises a single or multiple fault cores and a surrounding damage zone. The fault core is the main part of the fault and is composed of fault rocks (fault gouge, fault breccia, and cataclasite). The damage zone is an area in which the damage (joints, cracks, and small-scale faults) is greater than that in the surrounding country (host) rocks. Thus, such small-scale or minor faults are known to be densely developed near large-scale master faults (so-called "damage zones"; Chester and Logan 1987; Mitchell and Faulkner 2009). To define the extents of damage zones in the study area, we conducted a detailed survey across and on both sides of one of the Quaternary faults (the Unehata Fault; Fig. 7). The frequency (linear density) of minor faults shows a clear maximum (11 faults per 100 m) within 100 m of the Unehata Fault trace and decreases with increasing distance from the fault, being ≤ 1 fault per 100 m at > 500 m from the fault (Fig. 7). These results suggest the damage zone of the Unehata Fault extends ~ 500 m each side of the fault, similar to the Inagoe and Sugo Faults (the northeastern extension of the Toichigawa Fault) (Niwa et al. 2011). Therefore, we infer that the characteristic extent of the damage zone of Quaternary faults in the Inobuseyama area is ~ 500 m (i.e., total damage zone width of ~ 1000 m). We also infer that areas located > 500 m from the fault traces and geological faults are "background" areas in which the mechanical damage attributable to master faults is negligible.

The NKTZ trends NE–SW to ENE–WSW and shows dextral deformation, where the most of faults (Quaternary fault and minor faults) in this zone also strike NE–SW to ENE–WSW and record dextral slip. This correspondence of trend and displacement means that the dextral motion of the NKTZ can be obtained from the Quaternary faults in the zone. Moreover, the sense of movement of the NE–SW- to ENE–WSW-striking minor faults located outside of the damage zone (but within the NKTZ) is also dextral. On the other hand, all sinistral faults showed the NW–SE striking (nearly perpendicular to trend of the NKTZ), which indicates that the sinistral faults cannot either contribute to the dextral motion or negative motion of the NKTZ. The minor faults indicate a similar paleostress field to that of the present day (i.e., σ_1 trends E–W to ESE–WNW; σ_3 trends N–S to NNE–SSW; Fig. 9). Thus, we infer that the minor faults outside the damage zone are also active and contribute to the dextral motion of the NKTZ. The locations and trends of several faults measured in the Inobuseyama area are consistent with those of the fault traces and lineaments detected from aerial photographs (e.g., IF-5 in aerial photograph L44, IF-10 in L8, IF14 in L37, IF-15 in L50, and UF-1 to UF-7 in L48). This suggests that geologically recognized faults correspond to fault traces and lineaments detected from topographic features in aerial photographs. Fault traces and lineaments decrease in density with increasing distance from the central part of the NKTZ southeastward toward its margin (Fig. 14). However, outside of

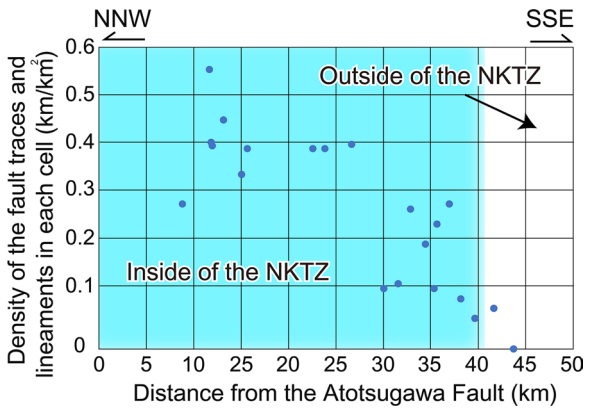

Fig. 14 Relationship between the areal density of the fault traces and lineaments (length of the traces per unit area) and distance from the Atotsugawa Fault. The total length of the fault traces and lineaments was measured in each of the 21 cells of the polygon enclosed by the red line in Fig. 3b. The pale-gray area in the graph depicts the area inside the NKTZ

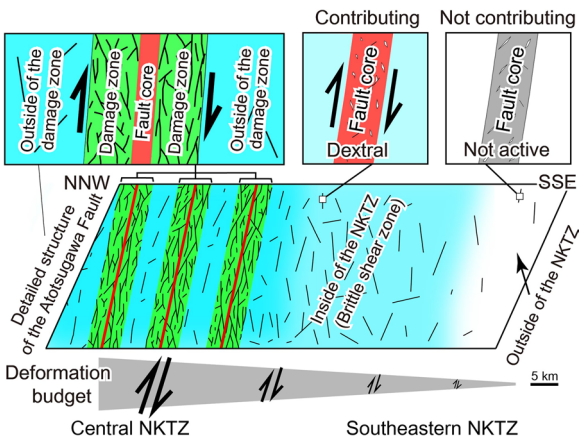

Fig. 15 Schematic model of deformation in the NKTZ. The thick red lines and green zones depict the fault core zones of major Quaternary faults and their damage zones, respectively. Blue areas with thin black lines represent an incipient brittle shear zone. Black arrows in the deformation budget show the inferred amount of dextral displacement contributed by faults in each area across the NKTZ

the NKTZ, minor faults are rarely recognized (only three faults in the Kurumijima area), apart from the geological faults. Within the NKTZ, in contrast, minor faults are commonly observed outside of damage zones (173 faults in the Inobuseyama area). The senses of shear and trends of minor faults outside of the NKTZ do not correspond to those within the NKTZ, implying that the former faults are not active and do not contribute to the dextral motion of the NKTZ. Therefore, combining the above observations, the hierarchical structure of deformation of the NKTZ can be summarized as follows (in order of decreasing deformation): (1) Quaternary faults, (2) damage zones of Quaternary faults, (3) zones of concentrated active minor faults (incipient brittle shear zones, or active background; these are beyond the damage zone but within the NKTZ), and (4) inactive background which is outside of the NKTZ (Fig. 15).

Conclusions

This study estimated the contribution of all faults to distributed deformation in the southeastern-central NKTZ. Accounting for deformation accommodated on minor faults and the corresponding slip rate allowed us to better constrain the deformation budget of the NKTZ. The major conclusions of the study are as follows:

1. An analysis of aerial photographs (1:10,000 to 1:20,000 scale) yielded 171 fault traces and lineaments in the southeastern-central NKTZ. The trends of these fault traces and lineaments are mainly NE–SW to ENE–WSW, consistent with the strike of the NKTZ. The density (length per unit area) of fault traces and lineaments increases toward the Atotsugawa Fault.
2. Minor faults in the Inobuseyama area trend NE–SW and are steeply dipping, and the movement on these faults is consistent with the present stress field. In contrast, faults in the Kurumijima area, located outside of the NKTZ, are mostly NE–SW to ENE–WSW trending with shallow to moderate plunging striations, and the movement on these faults is inconsistent with the present stress field and does not contribute to deformation in the NKTZ.
3. The total slip rate distributed across minor faults in the study area is estimated to be 0.46–2.88 mm/year. The total slip rate of all faults (including major and minor faults) in the southeastern-central NKTZ is estimated to be 7.2–9.6 mm/year, with this long-term slip constituting 60–80% of the total strain rate (12 mm/year) measured geodetically.
4. We identified a brittle shear zone (active background) that is characterized by concentrated minor faults.

Abbreviations

AGF: Atotsugawa Fault; AP: Amurian plate; ECSZ: eastern California shear zone; ENF: Enako Fault; GNSS: global navigation satellite system; GSI: Geospatial Information Authority of Japan; IHF: Inohana Fault; INF: Inagoe Fault; KDF: Kuchiudo Fault; NAP: North American plate; NKTZ: Niigata–Kobe Tectonic Zone; OSF: Osaka Fault; PP: Pacific plate; PSP: Philippine Sea plate; SKF: Shirakawa Fault; TGF: Toichigawa Fault; UHF: Unehata Fault.

Acknowledgements
We thank Dr. Takeshi Sagiya of Nagoya University for his helpful comments during the study. We also thank Dr. Kenta Kobayashi of Niigata University and Shun Suzuki of Graduate School of Niigata University for discussion regarding the Inagoe Fault outcrop.

Authors' contributions
TT conducted the topographic and geological surveys. KO, MO, AM, and MN conducted the geological survey. All authors contributed to data analysis, interpretation, and preparation of the paper. All authors read and approved the final manuscript.

Funding
This study was financially supported by the Fukada Grant-in-Aid of the Fukada Geological Institute. The Grant-in-Aid for Scientific Research on Innovative Areas (KAKENHI No. 2608) from MEXT, Japan.

Availability of data and materials
The datasets in the current study are available from the corresponding author on reasonable request.

Ethics approval and consent to participate
Not applicable to this study.

Consent for publication
Not applicable to this study.

Competing interests
The authors declare that they have no competing interests.

Author details
[1] Graduate School of Sciences and Technology for Innovation, Yamaguchi University, 1677-1, Yoshida, Yamaguchi 753-8511, Japan. [2] Geological Survey of Japan, National Institute of Advanced Industrial Science and Technology (AIST), 1-1-1 Higashi, Tsukuba 305-8567, Japan. [3] Tono Geoscience Center, Japan Atomic Energy Agency (JAEA), 959-31, Jorinji, Izumicho, Toki 509-5102, Japan.

Received: 3 October 2019 Accepted: 8 January 2020
Published online: 20 January 2020

References

Cello G, Roberto G, Stefano M, Andrew R, Emanuele T, Vittorio Z (2000) Fault zone characteristics and scaling properties of the Val d'Agri Fault System (Southern Apennines, Italy). J Geodyn 29:293–307. https://doi.org/10.1016/S0264-3707(99)00043-5

Chester FM, Logan JM (1987) Composite planar fabric of gouge from the Punchbowl Fault, California. J Struct Geol 9:809–817. https://doi.org/10.1016/0191-8141(87)90147-7

Childs C, Manzocchi T, Walsh JJ, Bonson CG, Nicol A, Schöpfer MPJ (2009) A geometric model of fault zone and fault rock thickness variations. J Struct Geol 31(2):117–127

Chuang RY, Johnson KM (2011) Reconciling geologic and geodetic model fault slip-rate discrepancies in Southern California: consideration of non-steady mantle flow and lower crustal fault creep. Geology 39(7):627–630. https://doi.org/10.1130/G32120.1

Dolan JF, Bowman DD, Sammis CG (2007) Long-range and long-term fault interactions in Southern California. Geology 35(9):855–858. https://doi.org/10.1130/G23789A.1

Fossen H (2010) Structural geology, vol 463. Cambridge University Press, Cambridge. https://doi.org/10.1017/CBO9780511777806

Gifu Prefecture (2001) Reports on active fault investigation of the Takayama-Oppara fault zones. https://www.hp1039.jishin.go.jp/danso/Gifu5Afrm.htm. Accessed 3 Oct 2019 **(in Japanese)**

Headquarters for Earthquake Research Promotion (HERP) (2004) Evaluation of the Takayama–Oppara fault zones. http://www.jishin.go.jp/evaluation/longtermevaluation/majoractivefault/. Accessed 30 July 2019 **(in Japanese)**

Iio Y, Sagiya T, Kobayashi Y, Shiozaki I (2002) Water-weakened lower crust and its role in the concentrated deformation in the Japanese Islands. Earth Planet Sci Lett 203(1):245–253. https://doi.org/10.1016/S0012-821x(02)00879-8

Ikeda Y, Okada S, Tajikara M (2012) Long-term strain buildup in the northeast Japan arc–trench system and its implications for gigantic strain-release events. J Geol Soc Jpn 118(5):294–312 **(in Japanese, with English abstract)**

Imanishi K, Kuwahara Y, Takeda T, Mizuno T, Ito H, Ito K, Wada H, Haryu Y (2011) Depth-dependent stress field in and around the Atotsugawa fault, central Japan, deduced from microearthquake focal mechanisms: evidence for localized aseismic deformation in the downward extension of the fault. J Geophys Res. https://doi.org/10.1029/2010jb007900

Isozaki Y, Maruyama S, Aoki K, Nakama T, Miyashita A, Otoh S (2010) Geotectonic subdivision of the Japanese Islands revisited: categorization and definition of elements and boundaries of Pacific-type (Miyashiro type) orogen. J Geogr 119(6):999–1053 **(in Japanese, with English abstract)**

Ito T, Tsumura N, Takeuchi A, Ishimuru T, Takami A, Ikawa H, Komada N, Yamamoto S, Miyauchi S, Kawanaka T, Ikawa T (2007) Imaging of the Mozumi-Sukenobe fault, Hida district, central Japan, by the seismic reflection method. In: Ando M (ed) Geodynamics of Atotsugawa Fault system. Tokyo, Terrapub

Itoh Y, Kimura H, Doshida S (2004) Active strike-slip faulting and macroscopically nonrigid deformation of volcanic rocks in central Japan inferred from a paleomagnetic study. Tectonophysics 374:81–98

Katsumata K, Kosuga M, Katao H, University Group of the Joint Seismic Observations at NKTZ (2010) Focal mechanisms and stress field in the Atotsugawa fault area, central Honshu, Japan. Earth Planets Space 62:367–380. https://doi.org/10.5047/eps.2009.12.006

Kimura H, Itoh Y, Tsutsumi H (2004) Quaternary strike-slip crustal deformation around an active fault based on paleomagnetic analysis: a case study of the Enako fault in central Japan. Earth Planet Sci Lett 226:321–334. https://doi.org/10.1016/j.epsl.2004.08.003

Matsuda T, Okada S, Watanabe T (2004) Development of active faults in Chugoku and Chubu districts—the comparison of cumulative slip, length of faults and width of crushed zones. Active Fault Res 24:1–12 **(in Japanese, with English abstract)**

Meneses-Gutierrez A, Sagiya T (2016) Persistent inelastic deformation in central Japan revealed by GPS observation before and after the Tohoku-Oki earthquake. Earth Planet Sci Lett 450:366–371. https://doi.org/10.1016/j.epsl.2016.06.055

Mitchell TM, Faulkner DR (2009) The nature and origin of off-fault damage surrounding strike-slip fault zones with a wide range of displacements: a field study from the Atacama fault system, northern Chile. J Struct Geol 31(8):802–816

Nakajima J, Hasegawa A (2007) Tomographic evidence for the mantle upwelling beneath southwestern Japan and its implications for arc magmatism. Earth Planet Sci Lett 254:90–105

Nakata T, Imaizumi T (2002) Digital active fault map of Japan. University of Tokyo Press, Tokyo **(in Japanese, with English abstract)**

Niwa M, Kurosawa H, Ishimaru T (2011) Spatial distribution and characteristics of fracture zones near a long-lived active fault: a field-based study for understanding changes in underground environment caused by long-term fault activities. Eng Geol 119(1–2):31–50

Nozawa T, Kawada K, Kawai M (1975) Geology of the Hida–Furukawa district. Quadrangle series scale 1:50,000. Geological Survey of Japan, Tokyo

Ohzono M, Sagiya T, Hirahara K, Hashimoto M, Takeuchi A, Hoso Y, Wada Y, Onoue K, Ohya F, Doke R (2011) Strain accumulation process around the Atotsugawa fault system in the Niigata–Kobe Tectonic Zone, central Japan. Geophys J Int. https://doi.org/10.1111/j.1365-246X.2010.04876.x

Oohashi K, Kobayashi K (2008) Fault geometry and paleo-movement of the central part of the Ushikubi fault, northern central Japan. J Geol Soc Jpn 114:16–30 **(in Japanese, with English abstract)**

Oohashi K, Otsubo M, Miyakawa A, Niwa M, Tamura T (2016) Geological and morphological features of the high-strain rate zone around the Atostugawa fault system, central Japan: distribution and nature of minor faults. In: Annual meeting, Geol Soc Jpn, R14-P1 **(in Japanese)**

Oskin M, Perg L, Shelef E, Strane M, Gurney E, Singer B, Zhang X (2008) Elevated shear zone loading rate during an earthquake cluster in eastern California. Geology 36(6):507–510. https://doi.org/10.1130/G24814A.1

Otsubo M, Sato K, Yamaji A (2006) Computerized identification of stress tensors determined from heterogeneous fault-slip data by combining the multiple inverse method and k-means clustering. J Struct Geol 28(6):991–997

Otsuki K, Uduki T, Monzawa N, Tanaka H (2005) Fractal size and spatial distributions of fault zones: an investigation into the seismic Chelungpu Fault, Taiwan. Isl Arc 14:12–21. https://doi.org/10.1111/j.1440-1738.2004.00454.x

Reid HF (1910) The California earthquake of April 18, 1906. Report of the State Earthquake Investigation Commission, vol 2, pp 16–18

Research Group for Active Faults of Gifu Prefecture (2008) Active faults in Gifu, Gifu Newspaper Gifu **(in Japanese)**

Research Group for Active Faults of Japan (1991) Sheet maps and inventories, Revised Edition. University of Tokyo Press, Tokyo **(in Japanese with English summary)**

Research Group for the Atotsugawa Fault, Okada A, Takeuchi A, Tsukuda T, Ikeda Y, Watanabe M, Hirfano S, Masumoto S, Takehana Y, Okumura K, Takumura T, Kobayashi T, Ando M (1989) Trenching study of the Atotsugawa Fault at Nokubi, Miyagawa Village, Gifu Prefecture, central Japan. J Geogr 98(4):62–85 **(in Japanese, with English abstract)**

Sagiya T, Meneses-Gutierrez A (2016) Crustal strain rate paradoxes of the Japan Islands: their resolution and implications. In: Taiwan–Japan Workshop: crustal dynamics 2016—Unified understanding of geodynamic processes at different time and length scales. July 19–22, Takayama, Japan

Sagiya T, Miyazaki S, Tada T (2000) Continuous GPS array and present-day crustal deformation of Japan. Pure Appl Geophys 157:2302–2322. https://doi.org/10.1007/PL00022507

Shipton ZK, Soden AM, Kirkpatrick JD (2006) How thick is a fault? Fault displacement–thickness scaling revisited. In: Abercrombie R (ed) Radiated energy and the physics of faulting. American Geophysical Union, Washington

Suzuki Y, Sugito N (2010) Sheet map of active faults in Gifu Prefecture, scale 1:50,000. Gifu Pref

Taira A (2001) Tectonic evolution of the Japanese Island arc system. Ann Rev Earth Planet Sci 29:109–134. https://doi.org/10.1146/annurev.earth.29.1.109

Takada K, Tanaka T, Nohara T, Haraguchi T, Ikeda Y, Ito K, Imaizumi T, Otsuki K, Sagiya T, Tsutsumi H (2003) Evoluation of active faults and lineaments as potential seismic faults in Chugoku district, Southwest Japan. Act Fault Res 23:77–91 **(in Japanese, with English abstract)**

Takeuchi A, Ongirad H, Takebe A (2003) Recurrence interval of big earthquakes along the Atostugawa fault system, central Japan: results of seismo-geological survey. Geophys Res Lett 30(6):8011. https://doi.org/10.1029/2002GL014957

Tsuneishi Y (1976) Fault related to the Gifuken-chubu Earthquake of September 9, 1969, in Central Japan. Geol Soci Jpn 12:129–137 **(in Japanese, with English abstract)**

Tsutsumi H, Sato K, Yamaji A (2012) Stability of the regional stress field in central Japan during the late Quaternary inferred from the stress inversion of the active fault data. Geophys Res Lett 39:L23303. https://doi.org/10.1029/2012GL054094

Wakita K (2013) Geology and tectonics of Japanese islands: a review—the key to understanding the geology of Asia. J Asian Earth Sci 72(10):75–87. https://doi.org/10.1016/j.jseaes.2012.04.014

Wesnousky SG, Scholz CH (1982) Deformation of an island arc: rates of moment release and crustal shortening in intraplate Japan determined from seismicity and quaternary fault data. J Geophys Res 87(B8):6829–6852

Yamada N, Adachi N, Kajita M, Harayama S, Yamazaki H, Bunno M (1985) Geology of the Takayama district. Quadrangle Series, scale 1:50,000. Geol Surv Jpn **(in Japanese, with English abstract)**

Yamaji A (2000) The multiple inverse method: a new technique to separate stresses from heterogeneous fault-slip data. J Struct Geol 22:441–452. https://doi.org/10.1016/S0191-8141(99)00163-7

Yamaji A, Sato K, Otsubo M (2011) Multiple inverse method software package user's guide. Kyoto University, Kyoto **(in Japanese with English version)**

Publisher's Note